JACS
JOURNAL OF THE AMERICAN CHEMICAL SOCIETY

Article

Hydrogen-Bonding and Hydrophobic Groups Contribute Equally to the Binding of Hyperactive Antifreeze and Ice Nucleating Proteins to Ice

Arpa Hudait, Yuqing Qiu, Nathan Odendahl, and Valeria Molinero

J. Am. Chem. Soc., **Just Accepted Manuscript** • DOI: 10.1021/jacs.9b02248 • Publication Date (Web): 25 Apr 2019

ACS Publications

is published by the American Chemical Society. 1155 Sixteenth Street N.W., Washington, DC 20036

Hydrogen-Bonding and Hydrophobic Groups Contribute Equally to the Binding of Hyperactive Antifreeze and Ice Nucleating Proteins to Ice

Arpa Hudait,[1] Yuqing Qiu,[1] Nathan Odendahl,[1] and Valeria Molinero[1*]

[1]Department of Chemistry, 315 South 1400 East, The University of Utah, Salt Lake City, Utah 84112-0580, USA

corresponding author, email: Valeria.Molinero@utah.edu

ABSTRACT. Hyperactive insect antifreeze proteins and bacterial ice-nucleating proteins are arguably the most potent ice-binding molecules in nature. These highly effective proteins bind ice through amphiphilic ice-binding sites based on arrays of threonine residues. It remains poorly understood how hydrophilic and hydrophobic groups of the binding site contribute to the ice affinity of proteins. Here we use molecular simulations to demonstrate that the hydrogen-bonding and hydrophobic groups at the ice-binding site of the antifreeze protein *Tm*AFP of *Tenebrio molitor* and extended ice-nucleating protein surfaces contribute distinctively yet almost equally in magnitude to their binding free energy to ice. The methyl groups rigidize the ice-binding site, slow down the water dynamics at the ice-binding surface, and stabilize the clathrate-like water in the anchored clathrate motif that binds these proteins to ice. We find that hydrophobic dehydration of the methyl group does not contribute to the binding free energy of the protein to ice. The role of the hydroxyl groups is to anchor the clathrate-like water through direct hydrogen-bonding, positioning and slowing down the dynamics of water at the trough of binding site. We uncover a correlation between slower dynamics of water at the binding site for the protein in solution and stronger free energy of binding of the protein to ice. The synergy between hydrophobic and hydrophilic groups unveiled by this study provides guidance for the design of synthetic ice-binding molecules with enhanced ice nucleation and antifreeze activity.

1. INTRODUCTION

A large variety of insects,[1-3] fish,[4-6] bacteria[7] and plants[8] that live at cold temperatures have evolved ice-binding proteins that either inhibit the growth or assist in the nucleation of ice. Interestingly, despite excelling at opposite functions, both hyperactive insect antifreeze proteins (AFPs) and bacterial ice nucleating proteins (INPs) bind ice through β-helices that contain TxT repeats, where T is threonine and x a non-conserved amino acid (Figure 1a).[1-3, 9] These repeats create a two-dimensional lattice-like arrangement with distances between hydroxyl groups comparable to those between water molecules in ice.[1] The repeating TxT sequences of AFPs and INPs bind ice through anchored clathrate (AC) motifs.[10-11] Water molecules in the AC motifs form a clathrate-like arrangement around the methyl groups of the threonine residues; these clathrate-like waters are anchored to the hydroxyl group of the protein through hydrogen-bonds (Figure 1c).[10-12] The AC motif of antifreeze and ice nucleating proteins with TxT binding sites is the same,[10] and similar to that first identified in the hydrated crystal of the hyperactive bacterial AFP *Mp*AFP, which also has an amphiphilic binding site.[7, 13]

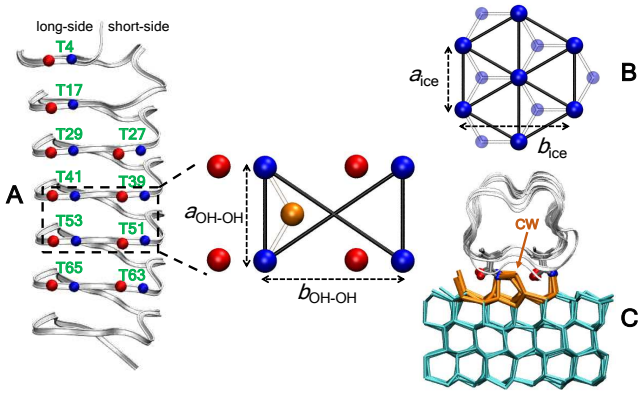

Figure 1. Ice-binding site (IBS) of the hyperactive insect AFP of *Tenebrio molitor*, *Tm*AFP. **a)** Threonine residues at the IBS are labeled in green. The methyl and hydroxyl groups of the threonine residues at the IBS are shown with red and blue balls, respectively. The protein backbone is shown with a silver ribbon. The IBS contains a row of 6 threonine residues (T4, T17, T29, T41, T53, T65), which we call the *long-side*, and a row with 4 threonine residues (T27, T39, T51, T63), which we call the *short-side*. The zoomed region shows also the position of a channel water (orange ball) in the inverted trough between the two rows of threonine residues. The distances between OH

groups in the protein, $b_{OH\text{-}OH}$ and $a_{OH\text{-}OH}$ are comparable to those in ice, parameters a_{ice} and b_{ice} in the basal plane of ice,[1] which is depicted in panel **b). c)** Snapshot of *Tm*AFP bound to the basal plane of ice. The anchored clathrate (AC) motif is shown with orange sticks, the ice with cyan sticks, and liquid water is hidden for clarity. The arrow indicates the position of the channel water (CW) molecules in the AC motif. All molecular images in the figures of this study are prepared with the software Visual Molecular Dynamics (VMD).[14]

It has been proposed that both hydrophobic and hydrogen-bonding interactions are needed for the recognition and binding of molecules to ice.[12, 15] However, some molecules such as antifreeze glycoproteins (AFGP) and type I AFPs bind ice using exclusively hydrophobic groups,[16-19] while others such as polyvinyl alcohol and long-chain alcohol monolayers bind ice exclusively through hydrogen-bonding groups.[20-21] Moreover, bacterial INPs, the most efficient ice nucleating molecules in nature, have two distinct binding sites, [9-10, 22-23] one amphiphilic and one hydrogen-bonding, which are equally efficient at binding ice.[10] Molecular simulations found significant differences in the hydration structure at the IBS of wild type *Tm*AFP and its mutant in which the OH group of 8 of the 10 Thr of the IBS is replaced by CH_3, emphasizing the important role of hydrogen-bonding and hydrophobic groups in the binding.[12] The relative contributions of hydrogen-bonding and hydrophobic moieties to the strength of binding of hyperactive AFPs and bacterial INPs to ice, however, have not yet been elucidated.

Experiments indicate that the antifreeze activity of the hyperactive insect AFPs *Tm*AFP and *Cf*AFP drastically diminishes when threonine residues at the ice-binding site are mutated to leucine, valine or alanine,[2, 24-26] which lack the ability to hydrogen bond to ice. Analogously, mutation of threonine of the IBS to arginine, histidine or tyrosine - which have hydrogen bonding but not methyl groups- results in proteins with complete or partial loss of antifreeze activity.[25] The diminished antifreeze activity of these mutants suggests that a synergism of hydrogen-bonding and hydrophobic moieties is essential for the strong binding of TxT based protein binding sites to ice.

A recent study has shown that the antifreeze activity of AFPs is correlated to the dynamics of interfacial water hydrating the protein: slower water dynamics at the IBS of AFP is associated with higher antifreeze activity.[27] Several past studies have reported slower dynamics of interfacial water at the IBS of hyperactive insect AFPs compared to the non-ice binding surface (non-IBS) of the protein.[27-32] In contrast to wild type insect AFPs, water at the IBS and non-IBS of protein mutants without antifreeze activity have comparable dynamics.[29, 31] An NMR study of the dynamics of water in the presence of *Tm*AFP reveals that the slowest water molecules at the IBS are the ones in the trough between the two rows of threonine residues.[33] The residence time of these channel waters (CW) was estimated to be about 0.3 ns.[33] We note that immobilization and ordering of the channel waters is fundamental to the mechanism of ice recognition of *Tm*AFP to ice.[10, 13] Simulations indicate that the interfacial water at the IBS attains the order of the AC motif only when *Tm*AFP is within 1 nm from the ice surface and with the axis of the binding site properly aligned with one of the ice axes.[13] The spontaneous ordering of the AC motif can also be facilitated by the slow dynamics of channel water at the IBS of hyperactive insect AFPs compared to the non-ice-binding site (non-IBS) of the protein.[27-32] The role of the hydrogen-bonding and hydrophobic residues in influencing the dynamics of channel water at the IBS remains unknown.

The molecular mechanism of ice recognition and binding by hyperactive antifreeze proteins is determined by multitude of factors: rigidity of the ice-binding site, water dynamics at the ice-binding site, and stability of the binding motif.[10, 13, 27, 34] Understanding how the interplay between the hydrogen-bonding and hydrophobic interactions at the ice-binding site modulate the aforementioned key elements of ice recognition and binding is the focus of this study. We use extensive molecular dynamics simulations with fully atomistic[35-36] and united-atom models[10, 37] to systematically investigate the role of the hydroxyl and methyl groups at the IBS proteins with TxT arrays in their binding sites on the rigidity of the binding site, the occupancy and residence time of channel water in solution, and their contributions to the binding free energy of this protein to ice. Our results indicate that hydrogen-bonding and hydrophobic groups play equally important and synergistic roles in the exceptional ice binding ability of proteins that bind ice with arrays of TxT amino acid sequences.

2. METHODS

2.1. Simulation Methods and Models.

We investigate the protein and its mutants through molecular dynamics simulations with all atom (AA) and united atom (UA) models. We build the models of wild type *Tm*AFP from the IEZG crystal structure available in Protein Data Bank.[1] Supporting Information A explains how we build the all-atom (Supp. Info A.1) and united-atom (Sup. Info. A.2) models, the cell dimensions, ensembles, simulation times, and simulation protocols. The all-atom proteins are modeled with CHARMM22 with CMAP correction,[36] solvated with TIP4P/2005 water,[35] same as in ref [10, 13]. The all-atom simulations of protein binding at the ice/water interface are performed at 246 K, 6±5 K below the melting point of the TIP4P/2005 model,[35] while simulations of the proteins in solution are performed at 273 K. Each all-atom simulation is ~200 ns long (Supp. Table S1). The length of the AA simulations is chosen to allow the spontaneous binding of proteins to the ice/water interface followed by at least 150 ns of sam-

pling, or –in the case of proteins in solution- to ensure that the mutant can repeatedly sample different conformations of the side chain at the ice-binding site (Supporting Section G). Supp. Info. A.1 provides the details of the AA models and simulations.

In the united-atom model, the proteins are represented with all atoms except hydrogen, using the models and force field of ref [10]. Water is modeled with the mW model,[37] which represents each water molecules as a single particle that interacts through two- and three-body interactions that mimic hydrogen bonds. Simulations with the mW model are over 100 times computationally more efficient than with fully atomistic rigid non-polarizable models of water with electrostatic interactions.[37] mW has been extensively validated for the modeling of the structure and thermodynamics of liquid water, ice, clathrates and their interfaces, as well as ice nucleation and the binding of antifreeze, ice nucleating and ice-recrystallization inhibitor molecules to the ice-liquid interface.[10, 13, 20-21, 37-62] The UA model of wild type *Tm*AFP is built from the crystal structure IEZG available in the Protein Data Bank,[1] scaling down the coordinates by 2%, as in ref [20], to maintain the experimental lattice mismatch to mW ice.

The UA *Tm*AFP is represented as either a single rigid body without internal fluctuations or a flexible model in which the united atoms are allowed to vibrate with harmonic springs around their crystallographic positions, with the spring parameters of ref [10]. The later model is only used to assess the role of flexibility on the residence times of channel water at the IBS of the wild type protein. The interactions between UA proteins and mW water are modeled with the Stillinger-Weber potential[63] with the parameters listed in ref [10]. The UA model of wild type *Tm*AFP reproduces the hydration structure in solution and the structure of the anchored clathrate motif in the bound state of the fully atomistic model of wild type *Tm*AFP.[10, 13] The UA mutant proteins are built from the rigid wild type *Tm*AFP by transforming the hydroxyl or methyl group of the threonine residues at the IBS and without allowing for structural relaxation of the protein. Supp. Info. A.2 provides the details of the UA models and simulations.

The spontaneous binding of the rigid united-atom proteins to ice is investigated through the evolution of *NpT* simulations at 272.5 K, 0.5 K below the melting point of the mW model,[37] for times that range from 100 to 300 ns. These simulations are detailed in Supp. Info A.2. Ice is identified with the CHILL+ algorithm.[64] To determine if a protein is bound to ice we monitor along the simulation trajectory the distance between the outmost ice layer (the layer below the ice/water interface) and the center of mass of the protein (Supporting Figure S1).

We use extended, periodic surfaces that repeat the UA rigid TCT sequence of amino acids with the same lattice mismatch to ice as *Tm*AFP, described in detail in the Supporting Information of ref [13]. Supporting Info. A2 provides the corresponding systems size and simulation detail. We use this surface for the calculation of the structure of interfacial water and heterogeneous nucleation temperature of ice as function of the size σ_{MW} and strength ε_{MW} of the interaction between methyl and water. We characterize the local structure of water with the Steinhardt bond-order parameter[65] q_3, averaged over the water molecules within 0.45 nm of the ice-binding surface of the protein (defined as the plane of the OH groups of the Thr residues). We compute this property as in ref [13] where we have shown that the value of q_3 can be used to distinguish ice, anchored clathrate, and liquid order at the surface of the proteins.[13] The heterogeneous ice nucleation temperatures are determined from simulations at constant cooling rate of 1 Kns^{-1} of the TCT surface in contact with water; the formation of ice is detected by the sudden drop of the potential energy of the system and verified through the identification of ice with the CHILL+ algorithm.[64] We then construct the response surface of the properties as a function of $\sigma_{MW} \bullet\bullet\bullet\bullet \varepsilon_{MW}$ using Uncertainty Quantification with generalized polynomial chaos, as in ref. [66] (Supp. Info. A.1).

2.2. Free energy calculations.

We calculate the binding free energy ΔG_{bind} of UA wild type *Tm*AFP and mutants to the basal plane of mW ice at 273 K using umbrella sampling (US) simulations. We perform the free energy calculations for the wild type and the mutants that spontaneously bind to ice in the up to 300 ns unconstrained simulations in two-phase ice/liquid cells. In the US simulations, the free energy profile is calculated as a function of the distance of the center of mass of the protein to the basal plane of ice, as in ref [10]. Supp. Info. A.3 details the umbrella sampling calculation of the free energy of binding of the proteins to ice.

We determine the free energy of binding per area of the periodic UA TCT surfaces to ice, from the parametric relation between the heterogeneous ice nucleation temperature and the binding free energy for mW at the nucleation rate of the cooling simulations, $J = 10^{27}$ cm^{-3} s^{-1}, neglecting the contribution of the ice-liquid-surface line tension to the nucleation barrier. [20, 67]

We compute the free energy of binding of methane to the basal and prismatic faces of ice at 273 K using umbrella sampling simulations with the M model of methane[59, 68] (which has the same interactions as the methyl groups of the proteins in our study), and mW water[37] following the same protocols used in ref [16] to compute these free energy profiles for all-atom models. We use thermodynamic integration to compute the free energy of hydration of UA methane groups

in liquid mW water at 273 K as a function of the size and strength of the interaction of the methane group with water, sampling the same set of sizes σ_{MW} and strengths ε_{MW} as for the periodic TCT surface. Supp. Info. D details the calculation of hydration free energies through thermodynamic integration.

2.3. Identification of the channel water molecules, and calculation of their residence time.

The channel water (CW) molecules are located in the inverted trough between rows of threonine residues, and are directly hydrogen-bonded to the hydroxyl group of the threonine residues on the long-side of the protein IBS (Figure 1).[1] We monitor the occupancy of water in the trough that are within 4.5 Å of both the hydroxyl and amide groups of two consecutive threonine amino acids (e.g. T53 and T65) on the long-side of the protein IBS. The same criterion is applied to identify the channel waters for the wild type, and the Thr→Ser and Thr→Val mutants. In the latter case, the distance criterion is applied with respect to the methyl and amide groups of the Val residues. We note that this criterion requiring the CW to be between two Thr identifies a maximum of 5 out of the 6 CW of the IBS of wild type *Tm*AFP. We assess the presence of the sixth CW through the density profile of water at the IBS. In ref [10] we used the same criterion to identify channel water described above, except that there we applied the criterion to only 4 threonine residues -T29, T41, T53, T65- which identifies a maximum of three channel water molecules. Supp. Info. A.4 details the calculation of the mean residence times of water molecules in the channel at the protein binding sites.

3. RESULTS AND DISCUSSION

3.1. The methyl groups of the threonine residues impart conformational rigidity to the ice-binding site.

Flatness and rigidity are key for strong binding of surfaces to ice.[20, 46-47] The β-helix secondary structures of hyperactive antifreeze proteins grant rigidity and flatness to their ice-binding sites.[69-71] The crystal structure of *Tm*AFP displays a narrow distribution of dihedral angles for the threonine residues, $\phi_{N\text{-}C\text{-}C\text{-}OH} = 57° \pm 3°$.[1] Experiments indicate that, also in solution, all threonine residues at the IBS of *Tm*AFP and its structural homolog *D*AFP-1 have identical orientation with respect to the backbone.[72-73] Experiments and all-atom simulations indicate that mutations of Thr to Val, which replace hydroxyl by methyl in the IBS of *Tm*AFP, preserve the orientation of the threonine residues at the IBS as in the wild type *Tm*AFP.[12, 25] It is not yet known, however, what is the effect of mutations of Thr to Ser, which eliminate the methyl group, on the conformational rigidity of TxT ice binding sites and how much this rigidity contributes to the binding free energy of the proteins to ice.

To investigate whether the methyl groups play a role in the conformational rigidity of the threonine residues at the IBS of *Tm*AFP, we mutate Thr53 at the IBS (Figure 1a) to serine, *i.e.* we remove a methyl group from the IBS, in the fully atomistic flexible protein model in solution. We find that the probability distribution of the dihedral $\phi_{N\text{-}C\text{-}C\text{-}OH}$ of the threonine residues in the wild type is unimodal, in agreement with NMR experiments of the protein in solution,[74] and centered around 60° (Figure 2a), close to the 57° ± 3° of the protein in the crystal.[1] This contrasts with the T53S mutant, in which $\phi_{N\text{-}C\text{-}C\text{-}OH}$ oscillates between 60° and 180° in both the solution and bound states, as it can be appreciated in the time evolution of the dihedral (Supp. Figure S7) and its bimodal probability distribution (Figure 2a). We conclude that the methyl groups of the threonine residues play a key role in maintaining the conformational rigidity of the threonine residues at the IBS of *Tm*AFP. The T53S mutant in solution favors the non-native $\phi_{N\text{-}C\text{-}C\text{-}OH} = 180°$ conformation over the native 60° by a free energy difference $\Delta G_{60°\to180°} = -RT \ln[P(180°)/P(60°)] = -6.1$ kJ mol^{-1} (Figure 2a), where P is the equilibrium probability of a given dihedral angle. We note that, despite the conformational flexibility of the IBS in solution, the mutant and wild type protein favor the same configurations in the ice-bound state (Figure 2a). This indicates that the flexibility of the Ser in the T53S mutant weakens the binding by 6.1 kJ mol^{-1}, the work needed to reposition the threonine from $\phi_{N\text{-}C\text{-}C\text{-}OH} = 180°$ to the wild type configuration of $\phi_{N\text{-}C\text{-}C\text{-}OH} = 60°$. We conclude that removal of the methyl groups of the threonine residues increases the flexibility of the binding site, weakening the binding of the protein to ice.

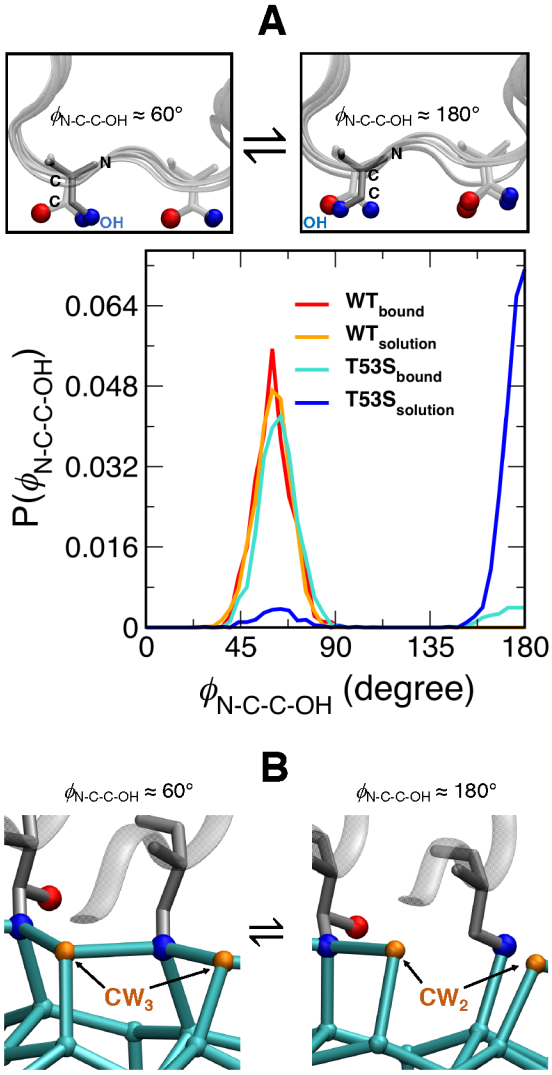

Figure 2. Effect of mutation of threonine to serine on the orientation of the hydroxyl groups of the ice-binding site of *Tm*AFP. **a)** The lower panel shows the probability distribution of $\phi_{N\text{-}C\text{-}C\text{-}OH}$ for residue 53 of wild type *Tm*AFP and T53S mutant. The distribution of $\phi_{N\text{-}C\text{-}C\text{-}OH}$ is centered around 60° for the wild type *Tm*AFP, both in solution and in the ice-bound state. In this conformation, the hydroxyl group points towards the trough between two rows of threonine residues. The distribution of $\phi_{N\text{-}C\text{-}C\text{-}OH}$ is bimodal in the T53S mutant, centered around 60° and 180° both in solution and in the ice-bound state. In solution Ser53 prefers the $\phi_{N\text{-}C\text{-}C\text{-}OH} \approx 180°$ conformation, the hydroxyl group pointing away from the trough. The upper panel shows the $\phi_{N\text{-}C\text{-}C\text{-}OH}$ conformations for Ser53 (solid gray sticks) relative to other threonine residues (transparent gray sticks) at the IBS. The hydroxyl and methyl groups of the residues at the IBS are shown with blue and red balls, respectively. The protein backbone is shown with a silver ribbon. The hydrogen atoms of protein and water are not shown. **b)** Structure of AC motif for ice-bound T53S mutant for $\phi_{N\text{-}C\text{-}C\text{-}OH} \approx 60°$ and 180° conformations shown in left and right panel respectively. The two nearest channel water molecules to Ser53 are shown with orange balls. All the water molecules are shown with cyan balls, and hydrogen-bonds are shown with cyan sticks. The rotation of the dihedral $\phi_{N\text{-}C\text{-}C\text{-}OH}$ from 60° to 180° breaks the hydrogen bond between the Ser53 hydroxyl and the closest channel waters. CW_3 and CW_2 denote channel waters closest to Ser53 hydroxyl in three- and two-coordinated states respectively. We note that for the ice-bound wild type *Tm*AFP the channel water is 3-coordinated, hydrogen bonded to the nearest two hydroxyl groups and a water molecule.[10]

3.2. Methyl groups are needed to stabilize the anchored clathrate that binds the protein to ice.

To elucidate whether the methyl groups have other role in the recognition and binding of the AFP to ice beyond rigidizing the IBS, we perform simulations in which we sequentially mutate the threonine residues to serine, and measure the binding free energy of each mutant to the basal face of ice. We model the wild type and mutants of *Tm*AFP at the UA level as a rigid body with the backbone structure of the wild type protein, solvated with mW water. The use of a rigid backbone for these mutants is justified, because serine and threonine residues have comparable β-sheet propensities.[75] To account for the cost of the loss of flexibility in the Thr→Ser mutants on the binding-free energy to ice, we first compute the free energy for the rigid mutants and then account for the destabilization due to the conformational flexibility by adding to it the reversible work to recover the native conformation, $\Delta G_{180°\to 60°} = 6.1$ kJ mol^{-1} per Ser at the IBS.

Figure 3 shows that the free energy of binding the protein to the basal plane of ice decreases steadily as the methyl groups are removed by mutation of Thr to Ser. Even without accounting for the loss in rigidity of the IBS, the mutated protein is unable to recognize and bind ice in up to 300 ns long unconstrained simulations when 8 or more of the 10 threonine residues of the conformationally ordered IBS have been replaced by serine. When the work of recovering the native $\phi_{N\text{-}C\text{-}C\text{-}OH} \approx 60°$ conformation for the OH groups at the IBS is accounted for, just 4 Thr→Ser mutations suffice to make the binding free energy unfavorable. We conclude that methyl groups play a key role in the molecular recognition and binding of *Tm*AFP to ice, and that this role goes beyond positioning the OH groups at the IBS.

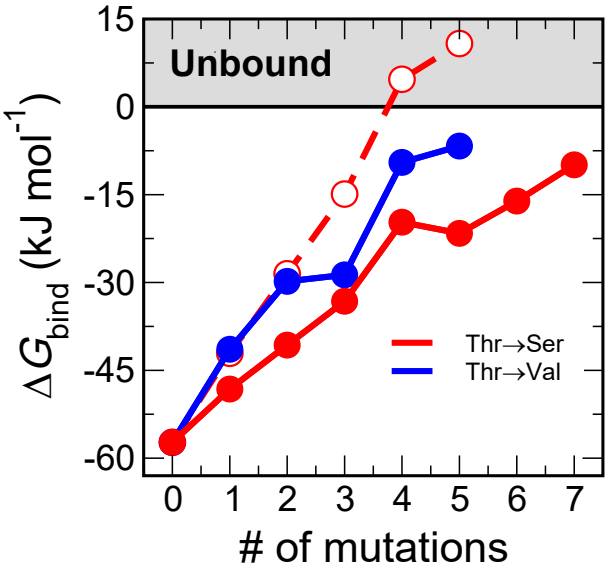

Figure 3. Contributions of the hydroxyl and methyl groups to ice affinity of *Tm*AFP, determined by the effect of mutations on the binding free energy of the protein to ice. Free energy of binding, ΔG_{bind}, of the rigid protein to the basal plane of ice at 273 K becomes less negative with the number of Thr→Ser (solid red circles) and Thr→Val (solid blue circles) mutations. The open red circles include the 6.1 kJ mol^{-1} cost per serine to recover the configuration with $\phi_{N\text{-}C\text{-}C\text{-}OH} \approx 60°$, needed to bind the OH group of the amino acid to ice. The order of the mutations is T29, T27, T39, T41, T53, T51, T63, T65, T17 and T4. Of these residues, T29, T41, T53, T65, T17 and T4 are in the long-side of the protein (Figure 1a), and T27, T39, T51 and T63 are in the short-side of the IBS (Figure 1a). The free energy of binding the wild type *Tm*AFP to the basal plane of ice is -57.3 kJ mol^{-1}.[10] Proteins with 8 or more Thr→Ser mutations or with 5 or more Thr→Val mutations do not bind to ice in up to 300 ns long unconstrained simulations, which suggests that they have $\Delta G_{bind} > 0$ (although we have not measured the binding free energies of these non-binding mutants).

We investigate the effect of mutating the threonine residues to serine, *i.e.* deleting the methyl groups, on the *short-side* and the *long-side* of the IBS (Fig. 1a). The methyl groups of the Thr of the long-side are in the outer boundary of the IBS, while those in the Thr of the short-side are in the inner side, between the two rows of OH groups. We find that mutations on these two sides of the IBS have distinct effects on the structure of the AC motif that binds the protein to ice. Deletion of the inner methyl groups in the short-side of the protein results in the formation of AC with empty clathrate-like cages when the protein is bound to ice. Guest-free cages are less stable than clathrate cages occupied by methane and other small hydrophobic guests,[76] resulting in a decrease in the magnitude of binding free energy (Figure 3). Removing methyl groups on the long-side of the protein does not lead to guest-free clathrate cages, but to the collapse of the clathrate-like water cages around the mutated residue. The collapse of the cages produces disordered water, incompatible with the underlying ice lattice, and, hence, also weakens the binding free energy of the mutant proteins (Figure 3). Our results are consistent with previous reports of stabilization of clathrate-like order induced by the adsorption of methane at the ice-like interface.[77-78] We conclude that a key role of the methyl groups in ice-binding proteins with TxT amino acid repeats is the ordering and stabilization of water into clathrate-like cages that form the AC motif that glues the protein to ice.

3.3. Hydrophobic dehydration does not drive the adsorption of TxT-based binding surfaces to ice.

Hydrophobic dehydration contributes to the binding of proteins to organic ligands and also to the stabilization of clathrate hydrates.[79-82] Hydrophobic dehydration is also responsible for the binding of AFGP and type I AFP to ice.[16, 19, 83] The hexagonal rings on the surface of ice provide shallow cavities wherein methane molecules or methyl groups can adsorb, freeing hydration water into the solution.[16] This results in modest entropy-driven free energies of adsorption of less than -2 kJ mol^{-1} per methane at the prismatic face and less than -0.5 kJ mol^{-1} per methane at the basal face for both the fully atomistic[16] and united atom models (Supporting Figure S2). The agreement among the UA and AA models in the free energy of binding of methane to ice, as well as in the free energy of hydrophobic attraction in water,[84-85] indicates that the united atom model can be used to assess the effect of hydrophobic interactions in the binding of the proteins to ice.

It has been hypothesized that hydrophobic dehydration provides the driving force for the binding of hydrophobic groups of the IBS of hyperactive insect antifreeze and bacterial ice nucleating proteins to ice.[34, 86-87] Proteins with TxT repeats in their binding sites, however, do not nest their methyl groups directly on the ice surface: they organize the interfacial water molecules into distinct anchored clathrate structures (Figure 1c). Experiments[33, 73] and simulations[13] indicate that water at the IBS does not have anchored-clathrate order when the protein is in solution. This implies that the interfacial water at the IBS must order to form the AC motif upon binding, *decreasing* the entropy. This analysis suggests that hydrophobic dehydration of the methyl groups at the IBS does not drive the binding of TxT-based protein binding surfaces to ice.

We estimate the entropy of binding of the united atom model of *Tm*AFP to ice from the temperature dependence of ΔG_{bind} and find it to be negative, ΔS_{bind} = -105 J K^{-1}mol^{-1} (Supporting Information C), disfavoring the binding. If the surface entropies of the AC/liquid and ice/liquid interfaces are identical, we use the latter[44] and a thermodynamic cycle to derive entropy associated to the formation of the AC at the IBS, which for *Tm*AFP has an area of 5.32 nm^2 (Support-

ing Information C). Our calculation indicates that the entropy of formation of the AC from solution would be about -386 $JK^{-1}mol^{-1}$. This corresponds to a loss of about -4 JK^{-1} per mole of water molecule in the AC motif. For comparison, the entropy loss upon formation of ice from water is about five times larger, -19.3 J $K^{-1}mol^{-1}$ for the mW model[37, 48] and -22.0 J $K^{-1}mol^{-1}$ in experiments.[88] The OH vibrational spectra of the AC is closer to that of liquid water than to that of ice,[13] indicating that the AC has higher entropy than ice. Nevertheless, the low entropy change involved in the formation of the AC motif from the liquid hydration water suggests that water at the surface of the binding site of the protein in solution has lower entropy, *i.e.* higher order, than in the bulk, despite the lack of AC of ice-like order at the binding site of the protein in solution. This conclusion is consistent with the finding of preferential locations for water molecules in the hydration shell of the protein in solution, as a recent study shows for *Tm*AFP with a fully atomistic model[12] and section 3.6 confirms for the united atom model. The lower entropy of water at the IBS may be associated to the slower dynamics of water at the IBS vs non-IBS of antifreeze proteins in solution,[27-32] which a recent study found to be correlated to a higher thermal hysteresis for a wide range of AFPs.[27]

It is known that propane forms more stable clathrates than methane.[89] As propane is more hydrophobic than methane, we investigate whether replacing the methyl groups at the IBS of *Tm*AFP by isopropyl strengthens the binding of the protein to ice. We replace the methyl groups of Thr27 and Thr29 in the rigid UA wild type *Tm*AFP by isopropyl groups, which have more favorable dehydration free energies than the methyl groups.[90] We find that the mutant binds to ice building the same AC motif as the wild type. The ΔG_{bind} of the double isopropylated mutant is, however, 20 kJ mol^{-1} (i.e. 35%) weaker than for wild type *Tm*AFP. This result, together with the overall increase in ordering of water around the hydrophobic groups to form the AC motif, suggest that the free energy of dehydration of hydrophobic groups at the IBS is not correlated to the binding free energy of the protein to ice.

Ice nucleating proteins have typically much larger ice-binding surfaces than antifreeze proteins, and they aggregate to form extended binding areas that stabilize the large ice crystallites required for ice nucleation at low supercooling.[67] Different from the small surfaces of AFPs, the large ice-binding surfaces of INP aggregates can induce clathrate-like order in the interfacial water at the IBS in contact with liquid water[11, 13] (Supporting Figure S3). We model the IBS of INP aggregates as an extended periodic surface that repeats rigid united atom TCT amino acid sequences (where C is cysteine) with the same mismatch to ice as in *Tm*AFP. To assess whether hydrophobicity of the IBS plays a role in the binding free energy of these surfaces to ice, we tune the hydrophobicity of the methyl groups by modulating the size σ_{MW} and strength ε_{MW} of the water-methyl interaction in the model. Figure 4 shows that there is no correlation between the hydration free energy of a methyl group in liquid water, $\Delta G_{hyd\ M}$, and the binding free energy per area of the IBS to ice, $\Delta G_{bind\ IBS}/A_{IBS}$, for the extended ice nucleating protein surfaces. This may not be surprising, as there is already quite developed AC-like order at these extended surfaces, hence the free energy of binding is dominated by the elimination of AC/liquid and ice/liquid interfaces. Together with our analysis for *Tm*AFP above, these results indicate that hydrophobic hydration does not drive the affinity of hyperactive insect AFPs and bacterial INPs to ice.

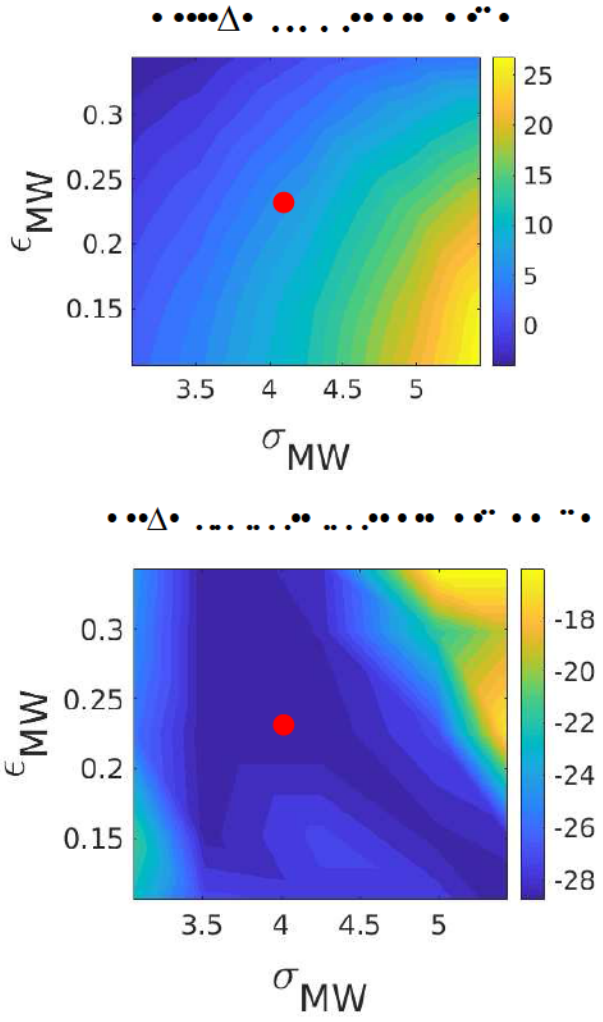

Figure 4. There is no correlation between hydrophobicity and binding free energy for extended ice-binding surfaces. Effect of the size σ_{MW} and strength ε_{MW} of attraction of the methyl M groups to water on a) the hydrophobic hydration of M, and b) ice-binding free energy per area of an ice-nucleating periodic rigid TCT surface with the same lattice mismatch to ice than *Tm*AFP. All properties computed with the united atom model. The red circle in each figure locates the parameters for the methyl group in the UA model of *Tm*AFP.

3.4. The methyl group of threonine has the optimum size to stabilize the anchored clathrate motif.

It is an open question whether it is possible to design proteins or synthetic molecules that bind to ice as strongly as hyperactive insect AFPs and bacterial INPs. The results of last section show that increasing the size of hydrophobic groups of the IBS from methyl to isopropyl diminishes the strength of binding of the protein to ice. Our analysis indicates that the weaker binding of the doubly isopropylated mutant is due to the strain that the large isopropyl groups exert on the water at the AC that binds the protein to ice: the average energy of water molecules in the AC is 2.4 ± 1.0 kJmol^{-1} higher when the IBS has isopropyl groups than when it has methyl groups. For reference, that quantity is almost half the enthalpy of melting of ice, 5.3 kJmol^{-1} for mW and 6.0 kJmol^{-1} for water.[37] We find the same qualitative results if the methyl groups are replaced by methyl-like moieties that are 35% larger and more hydrophobic than methyl (Supporting Information D). Our finding that larger hydrophobic groups weaken the ice-binding by *Tm*AFP mutants through steric effects is consistent with the lower antifreeze efficiency of mutants that replace threonine residues at the IBS to bulkier leucine, lysine and tyrosine in laboratory experiments.[71]

To understand why the isopropyl group does not form a more stable AC motif upon binding, despite propane forming more stable clathrates than methane, we note that these two alkanes form clathrates with different crystalline order: propane forms the sII clathrate crystal, which has larger water cages than the sI clathrate crystal formed by methane.[89] The isopropylated and wild type proteins, however, form identical AC. We conjecture that this is due to the constraints in the distances between the OH groups that anchor the protein to ice, which do not permit the formation of larger water cages that would better accommodate the isopropyl groups. Likewise, Supporting Figure S3 shows that the order of interfacial water at the IBS of large, periodic TCT surfaces in contact with liquid water and with the same mismatch to ice as *Tm*AFP, develop the highest extent of AC-like order when the size of the hydrophobic group in the threonine residues is close to that of the methyl group. Interestingly, we find that while the ordering of interfacial water at the extended IBS is very sensitive to the size of the hydrophobic group, it is quite robust against changes in its strength of interaction between with water. We conclude that the methyl group has the optimum size to stabilize the AC motif that binds hyperactive insect AFPs and bacterial INPs to ice.

3.5. Hydroxyl and methyl groups are both critical contributors to ΔG_{bind} of the protein to ice.

Having established the different roles that the methyl groups have on the binding of the protein to ice, we now focus on the role and contributions of the hydroxyl groups of the threonine residues to the binding. To this end, we perform sequential Thr→Val mutations of *Tm*AFP, each of which replaces an OH by a CH_3 at the IBS. We model the protein at the UA level as a rigid body, because both experiments and simulations with flexible models show that the IBS of these mutants preserves the β-helix secondary structure, flatness and rigidity of the wild type AFP.[12, 25]

We find that Thr→Val mutations steadily decrease the strength of binding of the protein to ice, as the hydrogen-bonding groups are sequentially mutated into methyl groups (Figure 3). The mutated protein is unable to bind ice in up to 300 ns long unconstrained simulations when 6 or more of the 10 Thr residues of the conformationally ordered IBS have been replaced by valine, suggesting that the ice-binding free energy of these mutants is positive (*i.e.,* unfavorable). This indicates that hydrogen-bonding by the hydroxyl groups is vital to build the clathrate-like order around the hydrophobic groups. Our results in Figure 3 are consistent with the weak thermal hysteresis activity exhibited by a mutant in experiments in which four Thr residues are substituted by valine.[25] The evolution of ΔG_{bind} upon sequential mutations of Thr to Ser or Val (Figure 3) reveal that both the hydroxyl and methyl groups are equally critical for determining the strength of binding of *Tm*AFP to ice.

3.6. Hydroxyl groups position the channel water and anchor clathrate-like water to the protein.

The TxT repeats at the binding site of *Tm*AFP produce a channel or trough between the two rows of threonine residues.[1] In the wild type, this channel is occupied by 6 water molecules, which have the slowest dynamics of the hydration shell of the protein.[33] The channel water is a key component of the AC motif that binds the protein to ice (Figure 1c).[10, 13] Figure 5 maps the probability density of interfacial water at the IBS of *Tm*AFP: the protein in solution has channel waters in the same positions as in the hydrated crystal[1] and in the AC motif of the ice-bound protein.[10] Supporting Figure S6 shows that hydration waters of the UA rigid *Tm*AFP model are in the same positions as in the fully atomistic flexible protein model of ref [12]. The channel waters are stabilized by hydrogen bonding to the OH groups of threonine residues on the long-side of the IBS (Figures 1c and 5a).[10, 12]

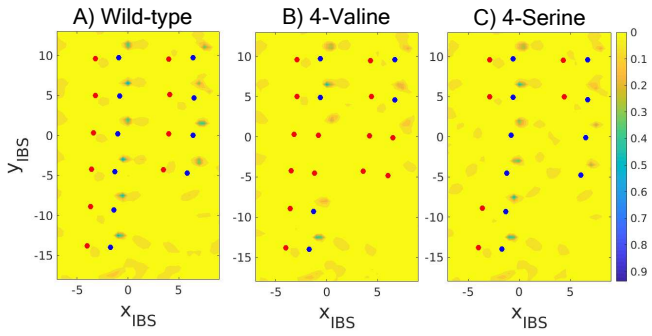

Figure 5. Density distributions of water molecules in contact with the IBS of (a) the wild type UA rigid *Tm*AFP protein, b) the mutant in which 4 Thr are mutated to Val, 4-Valine, and (c) the mutant in which 4 Thr are mutated to Ser, 4-Serine. The positions of the hydroxyl and methyl groups are shown with blue and red circles, respectively. The coloring of the density map indicates the probability of occupancy of water molecules; density of occupancy 1 indicates that the grid point is occupied by a water molecule in the entirety of the simulation time. The positions of the channel waters can be seen in light blue in the trough region, hydrogen bonded to the OH groups in the long-side of the IBS. Supporting Figure S5 presents the difference in density distribution between the mutants and wild type *Tm*AFP along the sequence of mutations.

The average number of channel water molecules N_{CW} sharply decreases with the number of Thr→Val mutations (Figures 5b and 6), as the OH groups that bind the channel waters are replaced by methyl groups. This indicates that secondary interactions with the backbone of the protein and the methyl groups are not sufficient to position the water molecules in the channel of the IBS. The water molecules in the protein trough are primarily stabilized by hydrogen-bonding to the nearest hydroxyl groups of the threonine residues.

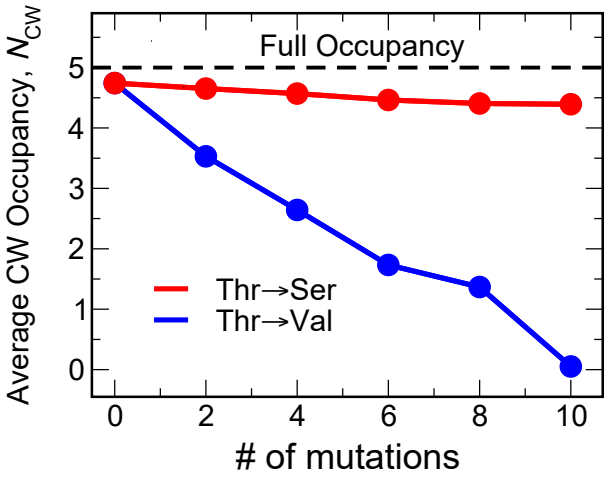

Fig. 6. Average occupancy of channel water N_{CW} as a function of the number of mutations for the rigid UA *Tm*AFP in solution at 273 K. We only monitor the 5 channel water molecules enclosed between pairs of OH groups in Figure 5. The order of the mutations is the same as in Figure 2. N_{CW} sharply decreases with the degree of mutation for Thr→Val substitution (solid blue line). N_{CW} is insensitive to the degree of mutation for Thr→Ser substitution (solid red line) in the rigid protein, but we nevertheless expect that the conformational flexibility of the OH in the flexible mutants will result in the loss of water in the channel (see Figure 2).

Interestingly, removal of the methyl groups through Thr→Ser mutations on the rigid protein model has little impact on the occupancy of the channel water molecules: Figures 5c and 6 show that the average number of channel waters N_{CW} in the trough decreases by less than one even when all Thr at the IBS of the rigid protein are mutated to Ser. This supports that the hydrogen bonding to the close OH of the IBS positions the water molecules in the protein trough. We note that although even when all threonine residues are mutated to serine in the rigid protein, the mutant protein (10-Ser) in solution retains occupancy of the water molecules in the channel but is unable to bind to ice. The lack of ice affinity of 10-Ser can be attributed to the asymmetric positioning of the middle row of channel waters, that offer a large lattice mismatch to ice, δb = -61%. This demonstrates that for asymmetrically positioned middle row of hydrogen-bonding group, as in TxT binding sites, the clathrate-like water arrangement around the hydrophobic groups plays a key role in building the AC motif that glues the protein to the ice surface.

Our results of section 3.1 indicate that the removal of the methyl groups upon a Thr→Ser mutation in the flexible protein results in the conformational change of the $\phi_{N\text{-}C\text{-}C\text{-}OH}$ dihedral from the native 60° to 180°. When $\phi_{N\text{-}C\text{-}C\text{-}OH}$ = 180°, the OH group cannot hydrogen bond to a water molecule in the channel, resulting in its dislocation (Figures 2b). Hence, we expect mutations of Thr to Ser on the long-side of the IBS (the one in which the hydroxyl groups bind the channel waters) in the flexible protein results in a significant decrease in the occupancy of water in the protein trough. We conclude that both Thr→Ser and Thr→Val mutations destabilize the water in the trough, and weaken the binding of the proteins to ice.

3.7. Immobilization of the channel water is correlated to strong binding of the protein to ice.

NMR experiments indicate that the channel water in the trough between the two rows of threonine residues has the slowest dynamics among all the hydration shell of the protein, with a residence time of about 0.3 ns at 293 K.[33] We determine the residence times of the CW in the flexible fully atomistic, UA flexible, and UA rigid protein models of wild type *Tm*AFP to be 0.11 ns, 0.3 ns and 1.3 ns, respectively, at 273 K (Supporting Table S2). The longer residence time of water solvating the rigid protein confirms that flexibility of the IBS is detrimental for the ordering of water in the channel.[10] It would be expected that the flexible united-atom model has a faster dynamics than the flexible all-atom model, as the diffusion coefficient of mW water model at 273 K is 5 times faster than that of TIP4P/2005.[37, 91] We attribute the shorter residence time of the flexible fully atomistic model to a slight lack of planarity of the IBS modeled with the CHARMM22 force field hydrated by TIP4P/2005 water.[10, 13] In what follows we focus on the relative effect of mutations of the rigid UA protein on the residence time of the channel water.

We find that Thr→Ser mutations on the rigid protein have a dramatic effect on the residence time of the channel waters (Figure 7), despite having very little impact on the average number N_{CW} of water molecules in the channel (Figure 5c and 6). This suggests that the slower dynamics of channel water in wild type *Tm*AFP is due to their confinement by neighboring methyl groups at the IBS. We note that the slowdown of water dynamics due to topological confinement is a general feature of water at interfaces.[92-94] We find a correlation between slower dynamics of water at the channel of the IBS and stronger binding of the protein to ice (inset of Figure 7). We expect the effect of these mutations on the occupancy and residence time of channel waters to be significantly more pronounced in the flexible mutant than determined in Figures 6 and 7 for the rigid mutants, as our fully flexible atomistic simulations indicate that the OH of the serine in mutants favors the $\phi_{N\text{-}C\text{-}C\text{-}OH}$ = 180° conformation that does not provide hydrogen bonding stabilization to water in the protein trough (Figures 2b).

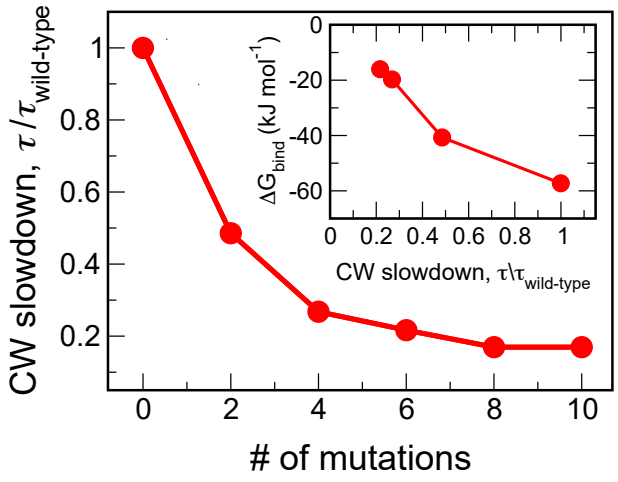

Figure 7. Slowdown of the residence time of water in the channel of the binding site as a function of the number of Thr→Ser mutations for rigid *Tm*AFP in solution at 273 K. The slowdown is defined as the ratio between the residence time τ of channel water normalized by the residence time of channel water for wild type *Tm*AFP for rigid UA protein, $\tau_{wild\ type}$ = 1.3 ns. The inset shows that the binding free energy for the wild type and rigid Thr →Ser mutants with up to 6 mutations is correlated with the dynamics of water in the trough of the IBS.

It is challenging to quantify the effect of hydroxyl groups on the residence time of channel water by analyzing the Thr→Val mutants, because the average number of channel water molecules, N_{CW}, monotonically decreases upon these mutations (Figures 5b and 6 and Supporting Figure S5). Instead, we quantify the influence of hydroxyl groups on the dynamics of channel water by systematically varying the strength of the hydrogen bond between the hydroxyl groups at the IBS and water, as the CW directly hydrogen-bond to the hydroxyl group of the nearest Thr residues. We tune the strength of the hydrogen bond by tuning the depth ε_{OHW} of the attraction between hydroxyl and water in the force field, as in ref. [20]. We find that the slowdown of the channel water, $\tau/\tau_{wild\ type}$, monotonically increases with the strength of the hydroxyl-water attraction (Figure 8). Most importantly, we find that the slower is the dynamics of the channel water, the stronger is the free energy of binding of the protein to ice (Figure 8 and inset of Figure 7).

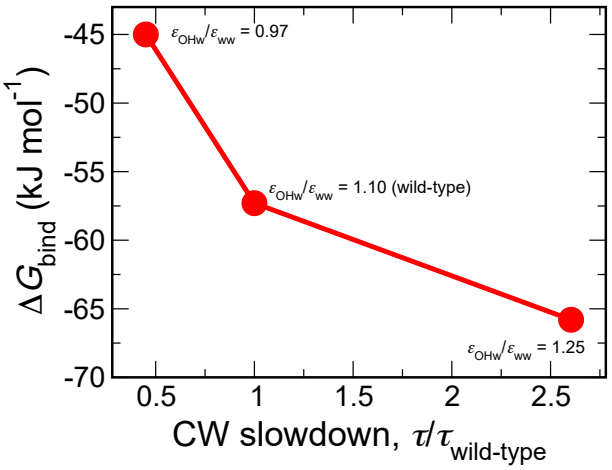

Figure 8. The free energy of binding of the protein to ice, ΔG_{bind}, becomes more negative and the slowdown of the channel water, $\tau/\tau_{wild\ type}$, more pronounced when the attraction between water and OH of the Thr of the IBS is strengthened with respect to the water-water attraction. The simulations are performed at 273 K for the rigid UA *Tm*AFP protein.

Stronger binding of proteins to ice increases their ice nucleation efficiency, $\Delta T_f = T_{het} - T_{hom}$, where T_{het} and T_{hom} are the temperatures of heterogeneous and homogeneous ice nucleation, respectively.[20, 67] Our analysis in Figure 8 suggests that deuteration of water or the OH of the threonine residues, which should increase the strength of hydrogen bonding[95-97] between the protein and its hydration shell, should increase the ΔT_f of proteins. This may contribute to the larger ice nucleation efficiency of *Tm*AFP in a mixture of light and heavy water, ΔT_f = 5 K,[33] and in light water, ΔT_f = 2.5 ± 2 K.[98] The predictions of simulations with the rigid UA model of *Tm*AFP in mW water are in quantitative agreement with the later, ΔT_f = 2 ± 1 K.[67] As strong binding to ice is also important for antifreeze activity,[53, 99-100] the correlation between slower dynamics of the CW and stronger binding of the protein to ice may explain why residence times at the IBS can be used to predict the magnitude of thermal hysteresis of antifreeze proteins.[27]

A recent computational study found that dispersion of hydrogen bonding groups on a surface reduces the mobility of interfacial water.[101] It may be expected that not all surfaces that slow down the dynamics of interfacial water are efficient at binding ice, because efficient binding to ice also requires

precise positioning of groups at the surface. It would be interesting to assess in future studies whether the principles uncovered in ref. [101] can be used to design effective ice-binding surfaces.

4. CONCLUSIONS

Hyperactive insect antifreeze protein and bacterial ice nucleating proteins bind strongly to ice through amphiphilic binding sites with TxT amino acid repeats.[20, 67] It has long been debated what is the role of hydrogen bonding and hydrophobic interactions in the binding of these proteins to ice.[2, 10-12, 102] In this work, we use fully atomistic and united atom molecular simulations to investigate the binding of large ice-nucleating TCT peptide surfaces and the hyperactive antifreeze protein *Tm*AFP, as well as mutants that result from systematic replacement of threonine residues at the binding site for valine, serine, and synthetic amino acids that modulate the hydrophobicity and hydrogen bonding strength of the binding surface. We find that the methyl and hydroxyl groups contribute equally to the ice-binding free energy of these exceptionally potent classes of antifreeze and ice nucleating proteins. To our knowledge, this is the first determination of the relative effect of hydrophobic and hydrogen bonding groups to the mode and strength of binding of these proteins to ice.

The simulations uncover synergistic effects of the hydrogen-bonding and hydrophobic groups at the IBS. We find that the methyl groups are key to maintain the conformational rigidity of the threonine residues at the IBS, ordering the OH and CH_3 groups into the positions needed for their binding to ice. When methyl groups are eliminated, the hydroxyl moiety of the resulting serine residues becomes rotationally flexible and unable to order and immobilize the water molecules in the trough of the binding site. The result is an entropic penalty to reorganize the hydroxyl groups and channel waters into their anchored clathrate configuration, which results in a significant weakening of the ice binding free energy.

The second role of the methyl groups is to order and stabilize water into a clathrate-like order, together with the anchoring hydroxyl groups, facilitating the formation of the anchored clathrate motif that glues the protein to the ice surface. Removal of methyl groups of the IBS results in disordered water cages or metastable guest-free clathrate cages in the bound state. Both yield a significantly less negative binding free energy. Our analysis indicates that methyl groups are optimally sized to stabilize the anchored clathrate; larger hydrophobic groups sterically strain the clathrate cages and reduce the binding efficiency.

We find that hydrophobic dehydration does not contribute to the binding of the proteins to ice. This is consistent with the increase in ordering of the water molecules around the methyl groups to form the anchored clathrate. Our thermodynamic analysis indicates that water at the binding surface of *Tm*AFP in solution has lower entropy than in bulk water, despite not presenting the order of ice or anchored clathrate.[13] This is consistent by the analysis of the density profiles of water molecules at the IBS of the protein, which show preferential positions for water molecules at the binding site, both in our analysis with united atom models and in fully atomistic simulations.[10-12] This positional order is particularly pronounced for water in the trough of the TxT binding surface. We find that the positioning and immobilization of the channel waters through hydrogen bonding to the closer hydroxyl groups of the threonine residues and their topological confinement by the methyl groups of the other row of threonine residues are key for the strong binding of the protein to ice.

We find a correlation between a slower dynamics of channel water and stronger ice binding strength of the protein. To our knowledge, this is the first time such correlation has been reported, and it may underlie the correlation between thermal hysteresis and dynamics of water at the binding site uncovered by a recent neural network analysis of antifreeze proteins.[27]. The correlation, however, may not be unexpected, as the relation between entropy and diffusivity in water is well documented,[103-105] and binding of the protein to ice requires immobilization and ordering of channel water, which would result in a penalty due to loss of entropy if water is not positioned in the channel or has high translational or rotational mobility. The positioning of the water molecules increases with the dimensions of the binding surface and is optimum for hydrophobic groups of the size of the methyl group. Proteins with properly positioned and slowly exchanging hydration water lose less translational entropy upon binding to ice, and therefore have stronger binding, which leads to more effective antifreeze[27, 53] and ice nucleation[20, 67] activities.

The analysis of this study suggests that the independently evolved TxT arrays of amino acids at the binding site of insect hyperactive antifreeze and bacterial ice nucleating proteins are thoroughly optimized for strong binding to ice: their chemical makeup ensure that they are rigid, flat, have the proper size of hydrophobic groups, and spacing of hydrogen bonding groups close to that of water molecules on ice. The elucidation in this study of the molecular contributions to the mode and strength of binding to ice of the most potent ice nucleating and antifreeze proteins evolved by nature paves the way for the rational design of more efficient synthetic mimics of these molecules for applications in cryopreservation,[106-108] food processing,[109] improving the freeze tolerance of plants, [110-111] and seeding of clouds to induce precipitation.[112]

Associated Content

Supporting Information. The Supporting Information is available free of charge on the ACS Publications website. The file contains supporting calculations and discussions, 6 Supporting Figures, and 2 Supporting Tables.

Acknowledgments

This work was supported by the National Science Foundation through award CHE-1305427 "Center for Aerosols Impacts on Chemistry and the Environment". We thank the Center for High Performance Computing at the University of Utah for technical support and a grant of computer time.

Author Information

Corresponding Author

Valeria.Molinero@utah.edu

Notes

The authors declare no competing financial interest.

References

(1) Liou, Y.-C.; Tocilj, A.; Davies, P. L.; Jia, Z., Mimicry of Ice Structure by Surface Hydroxyls and Water of a B-Helix Antifreeze Protein. *Nature* **2000,** *406*, 322-324.

(2) Graether, S. P.; Kuiper, M. J.; Gagné, S. M.; Walker, V. K.; Jia, Z.; Sykes, B. D.; Davies, P. L., B-Helix Structure and Ice-Binding Properties of a Hyperactive Antifreeze Protein from an Insect. *Nature* **2000,** *406*, 325.

(3) Hakim, A.; Nguyen, J. B.; Basu, K.; Zhu, D. F.; Thakral, D.; Davies, P. L.; Isaacs, F. J.; Modis, Y.; Meng, W., Crystal Structure of an Insect Antifreeze Protein and Its Implications for Ice Binding. *J. Biol. Chem.* **2013,** *288*, 12295-12304.

(4) Marshall, C. B.; Fletcher, G. L.; Davies, P. L., Hyperactive Antifreeze Protein in a Fish. *Nature* **2004,** *429*, 153.

(5) Sicheri, F.; Yang, D. S. C., Ice-Binding Structure and Mechanism of an Antifreeze Protein from Winter Flounder. *Nature* **1995,** *375*, 427.

(6) Jia, Z.; DeLuca, C. I.; Chao, H.; Davies, P. L., Structural Basis for the Binding of a Globular Antifreeze Protein to Ice. *Nature* **1996,** *384*, 285.

(7) Garnham, C. P.; Campbell, R. L.; Davies, P. L., Anchored Clathrate Waters Bind Antifreeze Proteins to Ice. *Proc. Natl. Acad. Sci.* **2011,** *108*, 7363-7367.

(8) Middleton, A. J.; Brown, A. M.; Davies, P. L.; Walker, V. K., Identification of the Ice-Binding Face of a Plant Antifreeze Protein. *FEBS Lett.* **2009,** *583*, 815-819.

(9) Garnham, C. P.; Campbell, R. L.; Walker, V. K.; Davies, P. L., Novel Dimeric B-Helical Model of an Ice Nucleation Protein with Bridged Active Sites. *BMC Struct. Biol.* **2011,** *11*, 36.

(10) Hudait, A.; Odendahl, N.; Qiu, Y.; Paesani, F.; Molinero, V., Ice-Nucleating and Antifreeze Proteins Recognize Ice through a Diversity of Anchored Clathrate and Ice-Like Motifs. *J. Am. Chem. Soc.* **2018,** *140*, 4905-4912.

(11) Midya, U. S.; Bandyopadhyay, S., Interfacial Water Arrangement in the Ice-Bound State of an Antifreeze Protein: A Molecular Dynamics Simulation Study. *Langmuir* **2017,** *33*, 5499-5510.

(12) Midya, U. S.; Bandyopadhyay, S., Role of Polar and Nonpolar Groups in the Activity of Antifreeze Proteins: A Molecular Dynamics Simulation Study. *J. Phys. Chem. B* **2018,** *122*, 9389-9398.

(13) Hudait, A.; Moberg, D. R.; Qiu, Y.; Odendahl, N.; Paesani, F.; Molinero, V., Preordering of Water Is Not Needed for Ice Recognition by Hyperactive Antifreeze Proteins. *Proc. Natl. Acad. Sci.* **2018,** *115*, 8266-8271.

(14) Humphrey, W.; Dalke, A.; Schulten, K., Vmd: Visual Molecular Dynamics. *J. Mol. Graph.* **1996,** *14*, 33-38.

(15) Schauperl, M.; Podewitz, M.; Ortner, T. S.; Waibl, F.; Thoeny, A.; Loerting, T.; Liedl, K. R., Balance between Hydration Enthalpy and Entropy Is Important for Ice Binding Surfaces in Antifreeze Proteins. *Sci. Rep.* **2017,** *7*, 11901.

(16) Mochizuki, K.; Molinero, V., Antifreeze Glycoproteins Bind Reversibly to Ice Via Hydrophobic Groups. *J. Am. Chem. Soc.* **2018,** *140*, 4803-4811.

(17) Haymet, A. D. J.; Ward, L. G.; Harding, M. M., Winter Flounder "Antifreeze" Proteins: Synthesis and Ice Growth Inhibition of Analogues That Probe the Relative Importance of Hydrophobic and Hydrogen-Bonding Interactions. *J. Am. Chem. Soc.* **1999,** *121*, 941-948.

(18) Nada, H.; Furukawa, Y., Growth Inhibition Mechanism of an Ice–Water Interface by a Mutant of Winter Flounder Antifreeze Protein: A Molecular Dynamics Study. *J. Phys. Chem. B* **2008,** *112*, 7111-7119.

(19) Sönnichsen, F. D.; DeLuca, C. I.; Davies, P. L.; Sykes, B. D., Refined Solution Structure of Type Iii Antifreeze Protein: Hydrophobic Groups May Be Involved in the Energetics of the Protein–Ice Interaction. *Structure* **1996,** *4*, 1325-1337.

(20) Qiu, Y.; Odendahl, N.; Hudait, A.; Mason, R.; Bertram, A. K.; Paesani, F.; DeMott, P. J.; Molinero, V., Ice Nucleation Efficiency of Hydroxylated Organic Surfaces Is Controlled by Their Structural Fluctuations and Mismatch to Ice. *J. Am. Chem. Soc.* **2017,** *139*, 3052-3064.

(21) Naullage, P. M.; Lupi, L.; Molinero, V., Molecular Recognition of Ice by Fully Flexible Molecules. *J. Phys. Chem. C* **2017,** *121*, 26949-26957.

(22) Maki, L. R.; Galyan, E. L.; Chang-Chien, M.-M.; Caldwell, D. R., Ice Nucleation Induced by Pseudomonas Syringae. *Appl. Microbiol.* **1974,** *28*, 456-459.

(23) Wu, Z.; Qin, L.; Walker, V. K., Characterization and Recombinant Expression of a Divergent Ice Nucleation Protein from 'Pseudomonas Borealis'. *Microbiology* **2009,** *155*, 1164-1169.

(24) Kuiper, M. J.; Morton, C. J.; Abraham, S. E.; Gray-Weale, A., The Biological Function of an Insect Antifreeze Protein Simulated by Molecular Dynamics. *eLife* **2015,** *4*, e05142.

(25) Bar, M.; Celik, Y.; Fass, D.; Braslavsky, I., Interactions of B-Helical Antifreeze Protein Mutants with Ice. *Cryst. Growth Des.* **2008,** *8*, 2954-2963.

(26) Lee, H., Effects of Hydrophobic and Hydrogen-Bond Interactions on the Binding Affinity of Antifreeze Proteins to Specific Ice Planes. *J. Mol. Graph. Model.* **2019,** *87*, 48-55.

(27) Kozuch, D. J.; Stillinger, F. H.; Debenedetti, P. G., A Combined Molecular Dynamics and Neural Network Method for Predicting Protein Antifreeze Activity. *Proc. Natl. Acad. Sci.* **2018**, 13252-13257.

(28) Duboué-Dijon, E.; Laage, D., Comparative Study of Hydration Shell Dynamics around a Hyperactive Antifreeze Protein and around Ubiquitin. *J. Chem. Phys.* **2014,** *141*, 22D529.

(29) Meister, K.; Ebbinghaus, S.; Xu, Y.; Duman, J. G.; DeVries, A.; Gruebele, M.; Leitner, D. M.; Havenith, M., Long-Range Protein-Water Dynamics in Hyperactive Insect Antifreeze Proteins. *Proc. Natl. Acad. Sci.* **2013,** *110*, 1617-1622.

(30) Nutt, D. R.; Smith, J. C., Dual Function of the Hydration Layer around an Antifreeze Protein Revealed by Atomistic Molecular Dynamics Simulations. *J. Am. Chem. Soc.* **2008,** *130*, 13066-13073.

(31) Xu, Y.; Gnanasekaran, R.; Leitner, D. M., Analysis of Water and Hydrogen Bond Dynamics at the Surface of an Antifreeze Protein. *J. At. Mol. Opt. Phys.* **2012,** *2012*, 125071.

(32) Lee, H., Structures, Dynamics, and Hydrogen-Bond Interactions of Antifreeze Proteins in Tip4p/Ice Water and Their Dependence on Force Fields. *PLOS ONE* **2018,** *13*, e0198887.

(33) Modig, K.; Qvist, J.; Marshall, C. B.; Davies, P. L.; Halle, B., High Water Mobility on the Ice-Binding Surface of a Hyperactive Antifreeze Protein. *Phys. Chem. Chem. Phys.* **2010,** *12*, 10189-10197.

(34) Davies, P. L., Ice-Binding Proteins: A Remarkable Diversity of Structures for Stopping and Starting Ice Growth. *Trends Biochem. Sci.* **2014,** *39*, 548-555.

(35) Abascal, J. L. F.; Vega, C., A General Purpose Model for the Condensed Phases of Water: Tip4p/2005. *J. Chem. Phys.* **2005,** *123*, 234505.

(36) MacKerell, A. D.; Bashford, D.; Bellott, M.; Dunbrack, R. L.; Evanseck, J. D.; Field, M. J.; Fischer, S.; Gao, J.; Guo, H.; Ha, S.; Joseph-McCarthy, D.; Kuchnir, L.; Kuczera, K.; Lau, F. T. K.; Mattos, C.; Michnick, S.; Ngo, T.; Nguyen, D. T.; Prodhom, B.; Reiher, W. E.; Roux, B.; Schlenkrich, M.; Smith, J. C.; Stote, R.; Straub, J.; Watanabe, M.; Wiórkiewicz-Kuczera, J.; Yin, D.; Karplus, M., All-Atom Empirical Potential for Molecular Modeling and Dynamics Studies of Proteins. *J. Phys. Chem. B* **1998,** *102*, 3586-3616.

(37) Molinero, V.; Moore, E. B., Water Modeled as an Intermediate Element between Carbon and Silicon. *J. Phys. Chem. B* **2009,** *113*, 4008-4016.
(38) Lu, J.; Qiu, Y.; Baron, R.; Molinero, V., Coarse-Graining of Tip4p/2005, Tip4p-Ew, Spc/E, and Tip3p to Monatomic Anisotropic Water Models Using Relative Entropy Minimization. *J. Chem. Theory Comput.* **2014,** *10*, 4104-4120.
(39) Moore, E. B.; Molinero, V., Structural Transformation in Supercooled Water Controls the Crystallization Rate of Ice. *Nature* **2011,** *479*, 506-508.
(40) Lupi, L.; Hudait, A.; Peters, B.; Grünwald, M.; Mullen, R. G.; Nguyen, A. H.; Molinero, V., Role of Stacking Disorder in Ice Nucleation. *Nature* **2017,** *551*, 218.
(41) Moore, E. B.; Molinero, V., Growing Correlation Length in Supercooled Water. *J. Chem. Phys.* **2009,** *130*, 244505.
(42) Moore, E. B.; Molinero, V., Ice Crystallization in Water's "No-Man's Land". *J. Chem. Phys.* **2010,** *132*, 244504.
(43) Qiu, Y.; Molinero, V., Why Is It So Difficult to Identify the Onset of Ice Premelting? *J. Phys. Chem. Lett.* **2018,** *9*, 5179–5182.
(44) Qiu, Y.; Lupi, L.; Molinero, V., Is Water at the Graphite Interface Vapor-Like or Ice-Like? *J. Phys. Chem. B* **2018,** *122*, 3626–3634.
(45) Shepherd, T. D.; Koc, M. A.; Molinero, V., The Quasi-Liquid Layer of Ice under Conditions of Methane Clathrate Formation. *J. Phys. Chem. C* **2012,** *116*, 12172-12180.
(46) Lupi, L.; Hudait, A.; Molinero, V., Heterogeneous Nucleation of Ice on Carbon Surfaces. *J. Am. Chem. Soc.* **2014,** *136*, 3156-3164.
(47) Lupi, L.; Hanscam, R.; Qiu, Y.; Molinero, V., Reaction Coordinate for Ice Crystallization on a Soft Surface. *J. Phys. Chem. Lett.* **2017,** *8*, 4201-4205.
(48) Hudait, A.; Qiu, S.; Lupi, L.; Molinero, V., Free Energy Contributions and Structural Characterization of Stacking Disordered Ices. *Phys. Chem. Chem. Phys.* **2016,** *18*, 9544-9553.
(49) Lupi, L.; Molinero, V., Does Hydrophilicity of Carbon Particles Improve Their Ice Nucleation Ability? *J. Phys. Chem. A* **2014,** *118*, 7330-7337.
(50) Hudait, A.; Molinero, V., What Determines the Ice Polymorph in Clouds? *J. Am. Chem. Soc.* **2016,** *138*, 8958-8967.
(51) Hudait, A.; Molinero, V., Ice Crystallization in Ultrafine Water–Salt Aerosols: Nucleation, Ice-Solution Equilibrium, and Internal Structure. *J. Am. Chem. Soc.* **2014,** *136*, 8081-8093.
(52) Johnston, J. C.; Molinero, V., Crystallization, Melting, and Structure of Water Nanoparticles at Atmospherically Relevant Temperatures. *J. Am. Chem. Soc.* **2012,** *134*, 6650-6659.
(53) Naullage, P. M.; Qiu, Y.; Molinero, V., What Controls the Limit of Supercooling and Superheating of Pinned Ice Surfaces? *J. Phys. Chem. Lett.* **2018,** *9*, 1712-1720.
(54) Lu, J.; Chakravarty, C.; Molinero, V., Relationship between the Line of Density Anomaly and the Lines of Melting, Crystallization, Cavitation, and Liquid Spinodal in Coarse-Grained Water Models. *J. Chem. Phys.* **2016,** *144*, 234507.
(55) Kastelowitz, N.; Johnston, J. C.; Molinero, V., The Anomalously High Melting Temperature of Bilayer Ice. *J. Chem. Phys.* **2010,** *132*, 124511.
(56) Johnston, J. C.; Kastelowitz, N.; Molinero, V., Liquid to Quasicrystal Transition in Bilayer Water. *J. Chem. Phys.* **2010,** *133*, 154516.
(57) Bullock, G.; Molinero, V., Low-Density Liquid Water Is the Mother of Ice: On the Relation between Mesostructure, Thermodynamics and Ice Crystallization in Solutions. *Faraday Discuss* **2013,** *167*, 371-388.
(58) Jacobson, L. C.; Hujo, W.; Molinero, V., Nucleation Pathways of Clathrate Hydrates: Effect of Guest Size and Solubility. *J. Phys. Chem. B* **2010,** *114*, 13796-13807.
(59) Jacobson, L. C.; Hujo, W.; Molinero, V., Amorphous Precursors in the Nucleation of Clathrate Hydrates. *J. Am. Chem. Soc.* **2010,** *132*, 11806-11811.
(60) Nguyen, A. H.; Jacobson, L. C.; Molinero, V., Structure of the Clathrate/Solution Interface and Mechanism of Cross-Nucleation of Clathrate Hydrates. *J. Phys. Chem. C* **2012,** *116*, 19828-19838.
(61) Nguyen, A. H.; Koc, M. A.; Shepherd, T. D.; Molinero, V., Structure of the Ice-Clathrate Interface. *J. Phys. Chem. C* **2015,** *119*, 4104-4117.
(62) Jacobson, L. C.; Molinero, V., Can Amorphous Nuclei Grow Crystalline Clathrates? The Size and Crystallinity of Critical Clathrate Nuclei. *J. Am. Chem. Soc.* **2011,** *133*, 6458-6463.
(63) Stillinger, F. H.; Weber, T. A., Computer Simulation of Local Order in Condensed Phases of Silicon. *Phys. Rev. B* **1985,** *31*, 5262-5271.
(64) Nguyen, A. H.; Molinero, V., Identification of Clathrate Hydrates, Hexagonal Ice, Cubic Ice, and Liquid Water in Simulations: The Chill+ Algorithm -. *J. Phys. Chem. B* **2015,** *119*, 9369-9376.
(65) Lechner, W.; Dellago, C., Accurate Determination of Crystal Structures Based on Averaged Local Bond Order Parameters. *J. Chem. Phys.* **2008,** *129*, 114707.
(66) Jacobson, L. C.; Kirby, R. M.; Molinero, V., How Short Is Too Short for the Interactions of a Water Potential? Exploring the Parameter Space of a Coarse-Grained Water Model Using Uncertainty Quantification. *J. Phys. Chem. B* **2014,** *118*, 8190-8202.
(67) Qiu, Y.; Hudait, A.; Molinero, V., How Do Size and Aggregation of Ice-Binding Proteins Control Their Ice Nucleation Efficiency. *J. Am. Chem. Soc.* **2019,** *DOI: 10.1021/jacs.9b01854*.
(68) Jacobson, L. C.; Molinero, V., A Methane−Water Model for Coarse-Grained Simulations of Solutions and Clathrate Hydrates. *J. Phys. Chem. B* **2010,** *114*, 7302-7311.
(69) Daley, M. E.; Spyracopoulos, L.; Jia, Z.; Davies, P. L.; Sykes, B. D., Structure and Dynamics of a B-Helical Antifreeze Protein. *Biochemistry* **2002,** *41*, 5515-5525.
(70) Graether, S. P.; Sykes, B. D., Cold Survival in Freeze-Intolerant Insects. *Eur. J. Biochem.* **2004,** *271*, 3285-3296.
(71) Marshall, C. B.; Daley, M. E.; Graham, L. A.; Sykes, B. D.; Davies, P. L., Identification of the Ice-Binding Face of Antifreeze Protein from Tenebrio Molitor. *FEBS Lett.* **2002,** *529*, 261-267.
(72) Daley, M. E.; Sykes, B. D., The Role of Side Chain Conformational Flexibility in Surface Recognition by Tenebrio Molitor Antifreeze Protein. *Protein Sci.* **2003,** *12*, 1323-1331.
(73) Meister, K.; Lotze, S.; Olijve, L. L. C.; DeVries, A. L.; Duman, J. G.; Voets, I. K.; Bakker, H. J., Investigation of the Ice-Binding Site of an Insect Antifreeze Protein Using Sum-Frequency Generation Spectroscopy. *J. Phys. Chem. Lett.* **2015,** *6*, 1162-1167.
(74) Daley, M. E.; Sykes, B. D., Characterization of Threonine Side Chain Dynamics in an Antifreeze Protein Using Natural Abundance 13c Nmr Spectroscopy. *J. Biomol. NMR* **2004,** *29*, 139-150.
(75) Minor Jr, D. L.; Kim, P. S., Measurement of the B-Sheet-Forming Propensities of Amino Acids. *Nature* **1994,** *367*, 660-663.
(76) Jacobson, L. C.; Hujo, W.; Molinero, V., Thermodynamic Stability and Growth of Guest-Free Clathrate Hydrates: A Low-Density Crystal Phase of Water. *J. Phys. Chem. B* **2009,** *113*, 10298-10307.
(77) Pirzadeh, P.; Kusalik, P. G., Molecular Insights into Clathrate Hydrate Nucleation at an Ice–Solution Interface. *J. Am. Chem. Soc.* **2013,** *135*, 7278-7287.
(78) Pirzadeh, P.; Kusalik, P. G., On Understanding Stacking Fault Formation in Ice. *J. Am. Chem. Soc.* **2011,** *133*, 704-707.
(79) Yagasaki, T.; Matsumoto, M.; Tanaka, H., Adsorption Mechanism of Inhibitor and Guest Molecules on the Surface of Gas Hydrates. *J. Am. Chem. Soc.* **2015,** *137*, 12079-12085.
(80) Baron, R.; Setny, P.; McCammon, J. A., Water in Cavity−Ligand Recognition. *J. Am. Chem. Soc.* **2010,** *132*, 12091-12097.
(81) Young, T.; Abel, R.; Kim, B.; Berne, B. J.; Friesner, R. A., Motifs for Molecular Recognition Exploiting Hydrophobic Enclosure in Protein–Ligand Binding. *Proc. Natl. Acad. Sci.* **2007,** *104*, 808.
(82) Bertolazzo, A. A.; Naullage, P. M.; Peters, B.; Molinero, V., The Clathrate–Water Interface Is Oleophilic. *J. Phys. Chem. Lett.* **2018,** *9*, 3224-3231.
(83) Wierzbicki, A.; Dalal, P.; Cheatham III, T. E.; Knickelbein, J. E.; Haymet, A.; Madura, J. D., Antifreeze Proteins at the Ice/Water Interface: Three Calculated Discriminating Properties for Orientation of Type I Proteins. *Biophys. J.* **2007,** *93*, 1442-1451.
(84) Song, B.; Molinero, V., Thermodynamic and Structural Signatures of Water-Driven Methane-Methane Attraction in Coarse-Grained Mw Water. *J. Chem. Phys.* **2013,** *139*, 054511.
(85) Baron, R.; Molinero, V., Water-Driven Cavity-Ligand Binding: Comparison of Thermodynamic Signatures from Coarse-Grained and Atomic-Level Simulations. *J. Chem. Theory Comput.* **2012,** *8*, 3696-3704.
(86) Jia, Z.; Davies, P. L., Antifreeze Proteins: An Unusual Receptor–Ligand Interaction. *Trends in Biochemical Sciences* **2002,** *27*, 101-106.
(87) Marks, S. M.; Patel, A. J., Antifreeze Protein Hydration Waters: Unstructured Unless Bound to Ice. *Proc. Natl. Acad. Sci.* **2018,** *115*, 8244.
(88) *Crc-Handbook Handbook of Chemistry and Physics, 81th Ed.; Crc: Boca Raton, 2000-2001.*
(89) Sloan Jr, E. D.; Koh, C., *Clathrate Hydrates of Natural Gases*. CRC press: New York, 2007.

(90) Ashbaugh, H. S.; Kaler, E. W.; Paulaitis, M. E., Hydration and Conformational Equilibria of Simple Hydrophobic and Amphiphilic Solutes. *Biophys. J.* **1998,** *75*, 755-768.
(91) Rozmanov, D.; Kusalik, P. G., Anisotropy in the Crystal Growth of Hexagonal Ice, Ih. *J. Chem. Phys.* **2012,** *137*, 094702.
(92) Fogarty, A. C.; Duboué-Dijon, E.; Laage, D.; Thompson, W. H., Origins of the Non-Exponential Reorientation Dynamics of Nanoconfined Water. *J. Chem. Phys.* **2014,** *141*, 18C523.
(93) Sterpone, F.; Stirnemann, G.; Laage, D., Magnitude and Molecular Origin of Water Slowdown Next to a Protein. *J. Am. Chem. Soc.* **2012,** *134*, 4116-4119.
(94) Laage, D.; Stirnemann, G.; Hynes, J. T., Why Water Reorientation Slows without Iceberg Formation around Hydrophobic Solutes. *J. Phys. Chem. B* **2009,** *113*, 2428-2435.
(95) Chen, B.; Ivanov, I.; Klein, M. L.; Parrinello, M., Hydrogen Bonding in Water. *Phys. Rev. Lett.* **2003,** *91*, 215503.
(96) Whalley, E., The Difference in the Intermolecular Forces of H2o and D2o. *Trans. Faraday Soc.* **1957,** *53*, 1578-1585.
(97) Calvin, M.; Hermans Jr, J.; Scheraga, H. A., Effect of Deuterium on the Strength of Hydrogen Bonds. *J. Am. Chem. Soc.* **1959,** *81*, 5048-5050.
(98) Eickhoff, L.; Dreischmeier, K.; Zipori, A.; Sirotinskaya, V.; Adar, C.; Reicher, N.; Braslavsky, I.; Rudich, Y.; Koop, T., Contrasting Behavior of Antifreeze Proteins: Ice Growth Inhibitors and Ice Nucleation Promoters. *J. Phys. Chem. Lett.* **2019,** *10*, 966-972.
(99) Sander, L. M.; Tkachenko, A. V., Kinetic Pinning and Biological Antifreezes. *Phys. Rev. Lett.* **2004,** *93*, 128102.
(100) Yagasaki, T.; Matsumoto, M.; Tanaka, H., Molecular Dynamics Study of Kinetic Hydrate Inhibitors: The Optimal Inhibitor Size and Effect of Guest Species. *J. Phys. Chem. C* **2018,** *123*, 1806–1816.
(101) Monroe, J. I.; Shell, M. S., Computational Discovery of Chemically Patterned Surfaces That Effect Unique Hydration Water Dynamics. *Proc. Natl. Acad. Sci.* **2018,** *115*, 8093-8098.
(102) Sharp, K. A., A Peek at Ice Binding by Antifreeze Proteins. *Proc. Natl. Acad. Sci.* **2011,** *108*, 7281-7282.
(103) Scala, A.; Starr, F. W.; La Nave, E.; Sciortino, F.; Stanley, H. E., Configurational Entropy and Diffusivity of Supercooled Water. *Nature* **2000,** *406*, 166.
(104) Nayar, D.; Chakravarty, C., Water and Water-Like Liquids: Relationships between Structure, Entropy and Mobility. *Phys. Chem. Chem. Phys.* **2013,** *15*, 14162-14177.
(105) Singh, M.; Dhabal, D.; Nguyen, A. H.; Molinero, V.; Chakravarty, C., Triplet Correlations Dominate the Transition from Simple to Tetrahedral Liquids. *Phys. Rev. Lett.* **2014,** *112*, 147801.
(106) Carpenter, J. F.; Hansen, T. N., Antifreeze Protein Modulates Cell Survival During Cryopreservation: Mediation through Influence on Ice Crystal Growth. *Proc. Natl. Acad. Sci.* **1992,** *89*, 8953-8957.
(107) He, Z.; Liu, K.; Wang, J., Bioinspired Materials for Controlling Ice Nucleation, Growth, and Recrystallization. *Acc. Chem. Res.* **2018,** *51*, 1082-1091.
(108) Biggs, C. I.; Bailey, T. L.; Ben, G.; Stubbs, C.; Fayter, A.; Gibson, M. I., Polymer Mimics of Biomacromolecular Antifreezes. *Nature Comm.* **2017,** *8*, 1546.
(109) Ustun, N. S.; Turhan, S., Antifreeze Proteins: Characteristics, Function, Mechanism of Action, Sources and Application to Foods. *J. Food Process Preserv.* **2015,** *39*, 3189-3197.
(110) Duman, J. G.; Olsen, T. M., Thermal Hysteresis Protein Activity in Bacteria, Fungi, and Phylogenetically Diverse Plants. *Cryobiology* **1993,** *30*, 322-328.
(111) Smallwood, M.; Worrall, D.; Byass, L.; Elias, L.; Ashford, D.; Doucet, C. J.; Holt, C.; Telford, J.; Lillford, P.; Bowles, D. J., Isolation and Characterization of a Novel Antifreeze Protein from Carrot (Daucus Carota). *Biochem. J.* **1999,** *340*, 385-391.
(112) Bruintjes, R. T., A Review of Cloud Seeding Experiments to Enhance Precipitation and Some New Prospects. *Bull. Am. Meteorol. Soc.* **1999,** *80*, 805-820.

TOC figure